Molecular Vision 2013; 19:2151-2164 <http://www.molvis.org/molvis/v19/2151>
Received 3 July 2013 | Accepted 29 October 2013 | Published 1 November 2013

sCD44 overexpression increases intraocular pressure and aqueous outflow resistance

Michael Giovingo,[1] Michael Nolan,[1] Ryan McCarty,[1] Iok-Hou Pang,[2,3,4] Abbot F. Clark,[3,4] Rachel M. Beverley,[1] Steven Schwartz,[1] W. Daniel Stamer,[5] Loyal Walker,[1] Algis Grybauskas,[1] Kevin Skuran,[1] Paulius V. Kuprys,[1] Beatrice Y.J.T. Yue,[1] Paul A. Knepper[1,6]

[1]Department of Ophthalmology and Visual Sciences, University of Illinois at Chicago, Chicago, Illinois; [2]Department of Pharmaceutical Sciences, University of North Texas Health Science Center, Fort Worth, TX; [3]Department of Cell Biology and Anatomy, University of North Texas Health Science Center, Fort Worth, TX; [4]North Texas Eye Research Institute, University of North Texas Health Science Center, Fort Worth, TX; [5]Department of Ophthalmology, Duke University Medical School, Durham, NC; [6]Department of Ophthalmology, Northwestern University Medical School, Chicago, IL

Purpose: CD44 plays major roles in multiple physiologic processes. The ectodomain concentration of the CD44 receptor, soluble CD44 (sCD44), is significantly increased in the aqueous humor of primary open-angle glaucoma (POAG). The purpose of this study was to determine if adenoviral constructs of CD44 and isolated 32-kDa sCD44 change intraocular pressure (IOP) in vivo and aqueous outflow resistance in vitro.

Methods: Adenoviral constructs of human standard CD44 (Ad-CD44S), soluble CD44 (Ad-sCD44), and empty viral cDNA were injected into the vitreous of BALB/cJ mice, followed by serial IOP measurements. Overexpression of CD44S and sCD44 was verified in vitro by enzyme-linked immunosorbent assay (ELISA) and western blot analysis. Anterior segments of porcine eyes were perfused with the isolated sCD44. sCD44-treated human trabecular meshwork (TM) cells and microdissected porcine TM were examined by confocal microscopy and Optiprep density gradient with western blot analysis to determine changes in lipid raft components.

Results: Intravitreous injection of adenoviral constructs with either Ad-CD44S or Ad-sCD44 vectors caused prolonged ocular hypertension in mice. Eight days after vector injection, Ad-CD44S significantly elevated IOP to 28.3±1.2 mmHg (mean±SEM, n=8; $p<0.001$); Ad-sCD44 increased IOP to 18.5±2.6 mmHg (n=8; $p<0.01$), whereas the IOP of uninjected eyes was 12.7±0.2 mmHg (n=16). The IOP elevation lasted more than 50 days. Topical administration of a γ-secretase inhibitor normalized Ad-sCD44-induced elevated IOP. sCD44 levels were significantly elevated in the aqueous humor of Ad-CD44S and Ad-sCD44 eyes versus contralateral uninjected eyes ($p<0.01$). Anterior segment perfusion of isolated 32-kDa sCD44 significantly decreased aqueous outflow rates. Co-administration of isolated sCD44 and CD44 neutralizing antibody or of γ-secretase inhibitor significantly enhanced flow rates. sCD44-treated human TM cells displayed cross-linked actin network formation. Optiprep density gradient and western blot analysis of human TM cells treated with sCD44 showed decreased annexin 2 expression and increased phosphorylated annexin 2 and caveolin 1 expression.

Conclusions: Our data suggest that sCD44 increases outflow resistance in vivo and in vitro. Viral overexpression of both CD44S and sCD44 is sufficient to cause ocular hypertension. Infusion of sCD44 in porcine anterior segment eyes significantly decreased flow rates. Notably, sCD44 enhanced cross-linked actin network formation. The elevated sCD44 levels seen in POAG aqueous humor may play an important causative role in POAG pathogenesis.

Primary open-angle glaucoma (POAG) is a common neurodegenerative disease characterized clinically by optic nerve damage and visual field loss. POAG is one of the four major causes of blindness and visual disability in the United States [1]. Elevated intraocular pressure (IOP) is a causative risk factor in POAG and the only treatable factor to date. One potential biologic marker of POAG is CD44, which is an adhesion/homing molecule. Direct evidence for CD44's role in POAG includes: 1) aqueous humor of POAG patients contains increased amounts of the soluble extracellular 32-kDa fragment of CD44 (sCD44) in comparison with the aqueous humor of age-matched normal individuals [2]; 2) increased levels of sCD44 in the aqueous correlates with the extent of visual field loss in POAG patients [3]; and 3) sCD44, particularly hypo-phosphorylated sCD44, is a potent and protein specifically toxic to trabecular meshwork (TM) cells [4].

CD44 is an 80 to 250-kDa transmembrane protein that is expressed in the majority of mammalian cell types. The CD44 ectodomain is released as sCD44 (Figure 1). CD44 is multifunctional due to sequence differences arising from alternate splicing of mRNA, as well as numerous post-translational modifications. CD44S (standard) is the most common form, comprising exons 1–5 and 15–19 [5]. CD44

Correspondence to: Paul A. Knepper, 150 East Huron, Suite 1000, Chicago, IL 60611; Phone: (312) 337-1285; FAX: (312) 337-1452; email: pknepper@northwestern.edu

splice variants containing variable exons are designated CD44v. CD44 proteins are differentially phosphorylated and glycosylated [6]. Notably, CD44S participates in the uptake and degradation of hyaluronic acid (HA) [7]. Ezrin, radixin, moesin (ERM) family members and ankyrin are located just beneath the plasma membrane and act as molecular linkers between the cytoplasmic domain of CD44 and actin-based cytoskeleton [8]. CD44 plays major roles in multiple physiologic processes including innate immunity [9], auto-immunity [10], phagocytosis [11], cell survival [12], and immunological synapses [13], and it functions as a "platform" for growth factors and matrix metalloproteinases (MMPs) including MT1-MMP, MMP-7, and MMP-9 [5]. The structure of CD44 is remarkable for its versatility. It is a molecule with a thousand faces due to its surprising number of functions, interactions, and alternate splicings [14].

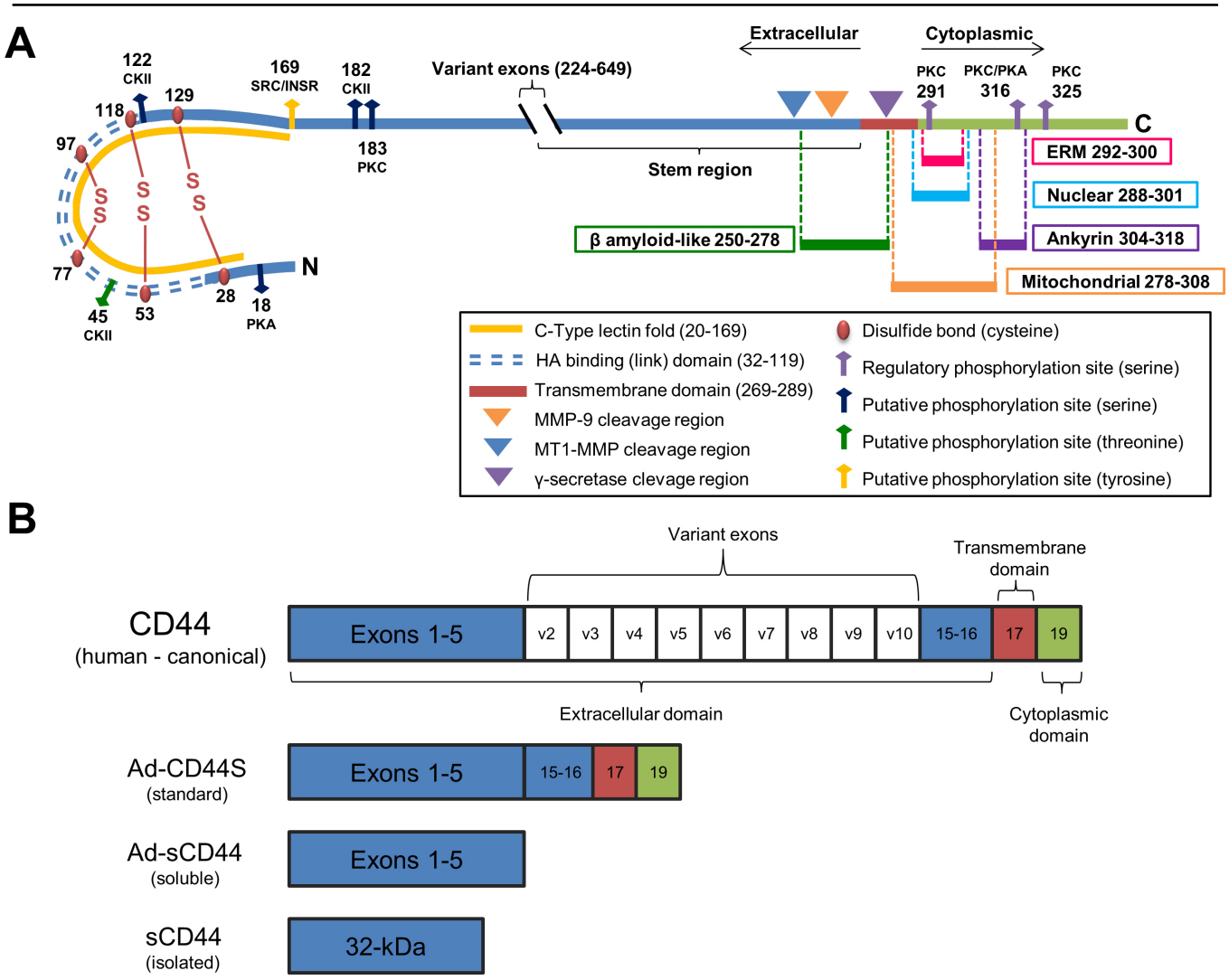

Figure 1. Schematic representation of CD44S. **A**: The extracellular (blue), transmembrane (red), and cytoplasmic (green) domains are illustrated for standard CD44S. The extracellular domain is characterized by cysteine residues that form disulfide bonds (maroon beads), including the two signature disulfide bonds that form the backbone of the link domain. Several extracellular putative phosphorylation sites as well as docking sites for MMP-9 and cleavages of CD44 by MT1-MMP (in conjunction with ADAMs 10 and 17) in the CD44 stem region and the transmembrane region by γ-secretase are shown. The cytoplasmic domain is characterized by three cytoplasmic phosphorylation sites (purple arrows) that modulate CD44 ezrin linking [46,47]. Note the extracellular β amyloid-like fragment and the nuclear and mitochondrial trafficking signals. Abbreviations for putative phosphorylation sites are: PKA, protein kinase A; PKC, protein kinase C; CKII, casein kinase II; SRC, sarcoma tyrosine kinase; INSR, insulin receptor kinase; ERM, ezrin, radixin, moesin. **B**: Gene structure of canonical CD44 with invariant exons 1–5, variable spliced exons 6–14, invariant exons 15–16 forming stem region, transmembrane exon 17, and cytoplasmic domain exon 19 is illustrated. Note exon 18 is spliced out [48]. Adenoviral constructs were the standard (Ad-CD44S) and truncated soluble (Ad-sCD44) isoforms; the isolated sCD44 is depicted for comparison to the constructs.

The sCD44 32-kDa ectodomain fragment of CD44 is released by proteolytic cleavage [7]. The sCD44 is shed from the cell surface in response to ligand binding. The ectodomain has been shown to be released from the cell surface by MT1-MMP, a membrane-bound MMP [15], in conjunction with ADAMS 10 and 17 [16]. The intramembrane portion of CD44 is cleaved by a presenilin γ-secretase at two sites: one cleavage occurs close to the cytoplasmic border to release an intracellular fragment that translocates to the nucleus and promotes transcription; a second cleavage occurs extracellularly to generate an amyloid-like peptide [17]. The purpose of this study was to test the effects of adenoviral constructs of CD44 on mouse IOP and the effects of isolated 32-kDa sCD44 in anterior segment perfusion cultures on aqueous outflow resistance.

METHODS

In vivo treatment of mice: All animals were treated in accordance with the ARVO Statement for the Use of Animals in Ophthalmic and Vision Research, and all protocols were approved and monitored by the Animal Care and Use Committee of Alcon Research, Ltd. BALB/cJ mice (2–5 months old; Jackson Laboratory, Bar Harbor, ME) used in this study were housed and handled as previously described [18].

Adenoviral vectors: Standard CD44 (CD44S) wild-type human CD44v4 cDNA (NM_001001391) was obtained from Origene (Rockville, MD) in the pCMV6-XL5 vector. sCD44 cDNA was produced by introducing a stop codon after exon 5 (Figure 1). The coding-region cDNAs were subcloned into the pacAdv.CMV.KN.pA shuttle vector (University of Iowa, Gene Transfer Vector Core) using EcoRI/Sba1 restriction digestion. Viruses were purified by CsCl gradient centrifugation, dialyzed against Tris-EDTA buffer containing 10% sucrose, and stored at −80 °C. Each virus was tested for wild type (WT) revertants and for titer by PCR and A549 plaque assay as previously described [18]. Empty adenovirus (Ad-Empty) was used as a negative control.

Adenovirus injection and intraocular pressure measurement: Adenoviral injection and IOP measurements were performed as previously described [18]. In brief, animals were examined at day −1 by direct ophthalmoscopy confirming a normal appearance, free of any signs of ocular disease. At day 0, mice were anesthetized and given a single 2 µl intravitreal viral vector injection (6×10^7 pfu/eye). IOP measurements were taken in conscious mice between 2 PM to 4 PM of the indicated days using a calibrated rebound tonometer (TonoLab; Tiolat Oy; Helsinki, Finland) as described [19]. A proprietary γ-secretase inhibitor (GSI, 1%w/v, Alcon Research, Ltd.) was topically applied to reverse the ocular hypertensive effects of Ad-CD44S. The IOP investigator was masked to all treatments.

Aqueous and tissue collection: At specified time points after adenoviral vector delivery, animals were euthanized with CO_2 asphyxiation. Aqueous humor of mice was obtained by paracentesis using a special designed glass microneedle. Three µl was slowly withdrawn from the anterior chamber from each eye and randomly assigned. An enzyme-linked immunosorbent assay (ELISA) assay measuring sCD44 concentrations was performed on samples of aqueous humor from human standard CD44 (Ad-CD44S)- and soluble CD44 (Ad-sCD44)-treated mouse eyes, as well as from their respective untreated contralateral eyes as previously described [20].

In vitro isolation of sCD44: sCD44 was sequentially isolated from human serum (Sigma-Aldrich, St. Louis, MO) using anion exchange chromatography, HA affinity chromatography, and immunoprecipitation as previously described [20]. The CD44 isolation was monitored at each step by determination of protein concentration (Bio-Rad, Hercules, CA) and sCD44 concentration by ELISA (Bender Medsystems, San Diego, CA) according to the manufacturer's instructions.

Perfusion of anterior segments: Porcine eyes (obtained fresh from a local abattoir and used within 4 h of death) were prepared using the Acott protocol [21]. In brief, prepared anterior segment caps were clamped into a perfusion apparatus with multiple ports, a small (1.5 mm) magnetic stir bar was placed in the anterior chamber, and serum-free Dulbecco's Modified Eagle's Medium (DMEM, Gibco, Grand Island, NY) was perfused at a constant pressure of 7.36 mmHg for 72 h using a reservoir system. To establish a stable baseline flow rate, the medium in the anterior chamber was briefly (15 s) mixed using a magnet, and the perfusate reservoir was then weighed every 30 min for three measurements to establish the baseline flow rates. The accepted normal flow rate for the porcine eye is 2–8 µl/min [22]. Individual anterior segments with unstable baselines or baselines outside the range of normal flow rates for porcine eyes were discarded. After a baseline flow rate was established, the medium in the anterior chamber was exchanged by simultaneously removing 1 ml of medium through one port, adding 1 ml of medium containing control solutions or test compounds through a second port, while maintaining the anterior chamber pressure at 7.36 mmHg via a third port. The anterior chamber exchange required approximately 2 min, and then the media in the anterior chamber was briefly mixed using the magnet. Subsequently, flow rates were measured over multiple time points and the anterior chamber was stirred using the magnet after each flow measurement. The neutralizing sCD44

antibody was monoclonal BU52 antibody (Ancell, Bayport, MN), and a proprietary γ-secretase inhibitor was supplied by Alcon Research.

To facilitate comparison between treatments, normalized flow rates were calculated by dividing the actual flow rate at each time point for each eye by the average baseline flow rate for that eye before the anterior chamber exchange. Time point "0" represents the average baseline flow rate before the start of anterior exchange. Flow rate was the change in the weight of the reservoir assuming the specific gravity of the perfusate to be 1.0.

Western blot and lipid raft profiles: TM cells were isolated using the Stamer method [23] and were treated with 1 ng of 32-kDa sCD44 for 24 h as previously described [20]. The porcine TM was microdissected from the corneal scleral ring after 72 h of continuous perfusion with 1 ng/ml of 32-kDa sCD44. Proteins of cell lysates of human TM cells and porcine TM treated with 32-kDa sCD44 were separated by an Optiprep density gradient according to the manufacturer's instructions (Sigma-Aldrich). Human TM cells were grown in DMEM containing 10% fetal bovine serum (FBS) until confluent. The cells were washed twice with PBS, and incubated in DMEM containing 0.1% FBS with 0.1 ng sCD44 or PBS control for 24 h. The medium was aspirated. The cells were washed with cold PBS, subjected to lysis buffer (Sigma-Aldrich) containing 1% Triton X-100 and 1% protease inhibitor cocktail (Sigma-Aldrich), scraped from the flask and collected. The TM of the perfused porcine eye was microdissected and placed into lysis buffer containing 1% Triton X-100. The preparations were centrifuged at 200,000 ×g for 18 h, and nine 1.0 ml fractions were collected from the top (lightest) to the bottom (heaviest). Each fraction was analyzed for protein content (Pierce Biotechnology, Rockford, IL), resolved by SDS PAGE, and immunoblotted with anti-caveolin-1 (Sigma-Aldrich), anti-caveolin-2 (Sigma-Aldrich), anti-annexin 2 (Santa Cruz Biotechnology, Dallas, TX), and anti-annexin 2 phosphorylated (Santa Cruz Biotechnology) antibodies. Densitometry analysis was performed on the western blots of the lipid raft proteins. Mean intensity was determined and background values as well as nonspecific staining of the secondary antibodies were subtracted to obtain the total amount of primary antibody staining using MetaMorph® Version 7.5.6.0 (MDS Analytic Technologies, Sunnyvale, CA). Data were normalized to positive staining of Jurkat cell lysates (Santa Cruz Biotechnology).

Immunofluorescence and actin staining: Primary cultures of TM cells derived from donors of 19, 34, and 49 years of age were plated at 5,000 cells per well on 8-well chamber slides in DMEM containing 10% FBS as previously described [20]. The medium was changed to 0.1% FBS for 2 h before treatment. The isolated 32-kDa sCD44 (0.1 ng) was added to the wells, and the slides were incubated at 4 °C for 1 h. Excess 32-kDa sCD44 not bound to the cell surface was removed by aspiration, fresh medium was added, and the slides were incubated for another 2 h at 37 °C. The cells were rinsed 3 times with PBS at room temperature, fixed using 3.7% formaldehyde at room temperature for 10 min, and then rinsed 2 times with PBS. Cells were incubated for 90 min with a mouse anti-annexin 2 antibody or phosphorylated annexin 2 antibody (dilution 1:500, Santa Cruz). The cells were then washed and incubated for 45 min with secondary FITC-labeled goat antimouse antibody (diluted 1:200 in 10% normal goat serum; Jackson ImmunoResearch, West Grove, PA). The cells were rinsed three times with PBS and stained for actin using 150 µl of Actin Stain (45 µl rhodamine phalloidin [Life Technology, Carlsbad, CA]; 1750 µl PBS; 5 µl 1% bovine serum albumin [BSA; Bio-Rad]) at room temperature for 25 min. The cells were rinsed and mounted with Vectashield with DAPI (Vector, Burlingame, CA). The staining was visualized with a 100× oil immersion objective and Leica SP2 confocal microscope (Wetzlar, Germany).

The percent of filamentous actin (F-actin) that exhibited cross-linked actin network (CLAN)-like characteristics within a specific cell (the vertices of the actin defined as the ends of F-actin or hubs of F-actin from which other F-actin bundles branch off) were identified and counted as either exhibiting regular formation or CLAN-like formation if at least three vertices were connected with strongly fluorescent F-actin spokes. The image was partitioned into a 3×3 grid and the vertices were counted following a regular pattern on the grid until at least 100 vertices were counted.

Statistical analysis: Data were presented as mean ± SEM. Student's t-test was used to compare two groups of results. One-way analysis of variance (ANOVA) followed by Dunnett's test was used to compare three or more groups. A p value of <0.05 was regarded as statistically significant, calculated by statistical analysis software (Prism 4 [GraphPad Software, La Jolla, CA] or SigmaPlot 10 [Systat Software, Inc., Chicago, IL]).

RESULTS

Effects of adenoviral vectors on CD44 levels in human trabecular meshwork cells: Adenovirus vectors Ad-CD44S, Ad-sCD44, and Ad-empty were used to infect human TM cells (Figure 1). To determine if the adenoviral vectors were active in vitro, transfected human TM culture media and cell lysates were analyzed for CD44 levels by ELISA (Figure 2). In all cases, there was a greater amount of CD44 in TM cell

lysates than in the media. The Ad-sCD44 CD44 concentration was significantly greater than Ad-CD44S ($p<0.01$). CD44 concentration was 37.3 (±5.0) ng/ml in the media of Ad-CD44S-treated TM cultures and was 221.7 (±0.5) ng/ml in cell lysates. The corresponding CD44 concentrations in Ad-sCD44 treated cultures were 154.3 (±6.6) and 172.5 (±2.0) ng/ml respectively. In Ad-empty-treated cultures, the CD44 concentration was 26.1 (±8.6) ng/ml in the media and 128.3 (±1.9) ng/ml in cell lysates (Figure 2). Using human serum as a positive control for the ELISA assay—human serum was 794.9 (±28.4) ng/ml and 1% FBS as a negative control—the FBS was 2.8 (±0.4) ng/ml. Also, to determine if the adenoviral vectors were active in vitro, western blot analysis was used to confirm the ELISA determinations of cell lysates and media and to determine the expression of CD44. A prominent 64-kDa, a dimer of the 32-kDa sCD44, was present in the three adenovirus-treated cells. See Figure 3. In both the Ad-sCD44 and Ad-CD44S cell lysates, the staining intensity of the western blot was greater than Ad-empty cell lysates. The 64-kDa band in adenovirus-treated cells was also observed in the human serum, 1% FBS and exogenenous 32-kDa sCD44.

ELISA determinations were also used to measure CD44 in the aqueous humor of adenovirus-transduced mouse eyes (Figure 4). In Ad-CD44s-treated eyes, the CD44 concentration was 138.5 (±72.1) ng/ml. In the uninjected contralateral eyes, the mean concentration of CD44 was 9.1 (±7.8) ng/ml. In Ad-sCD44 eyes, the ELISA CD44 concentration was 150.1 (±39.8) ng/ml. In the uninjected contralateral eyes, the mean concentration of CD44 was 0.2 (±0.1) ng/ml (Figure 4).

Effect of adenoviral overexpression of CD44 on mouse intraocular pressure: On the basis of ELISA concentrations, adenovirus treatment resulted in overexpression of CD44 in TM cells and in mouse eyes. Therefore, we tested the effects of three adenoviral constructs on IOP in mice (Figure 5). An increase in IOP was observed within 4 days. Variable time-dependent peaks in IOP were observed with the Ad-CD44s-treated eyes. One peak in IOP to 28 mmHg occurred at 14 days. Two more peaks were observed, one at 30 days (24 mmHg) and the other at 50 days (29 mmHg). Similarly, variable time-dependent peaks of increased IOP were observed with Ad-sCD44 although the increase was less than the Ad-CD44S-treated eyes. An onset of increased IOP was observed at day 8, reached at a peak of 22 mmHg

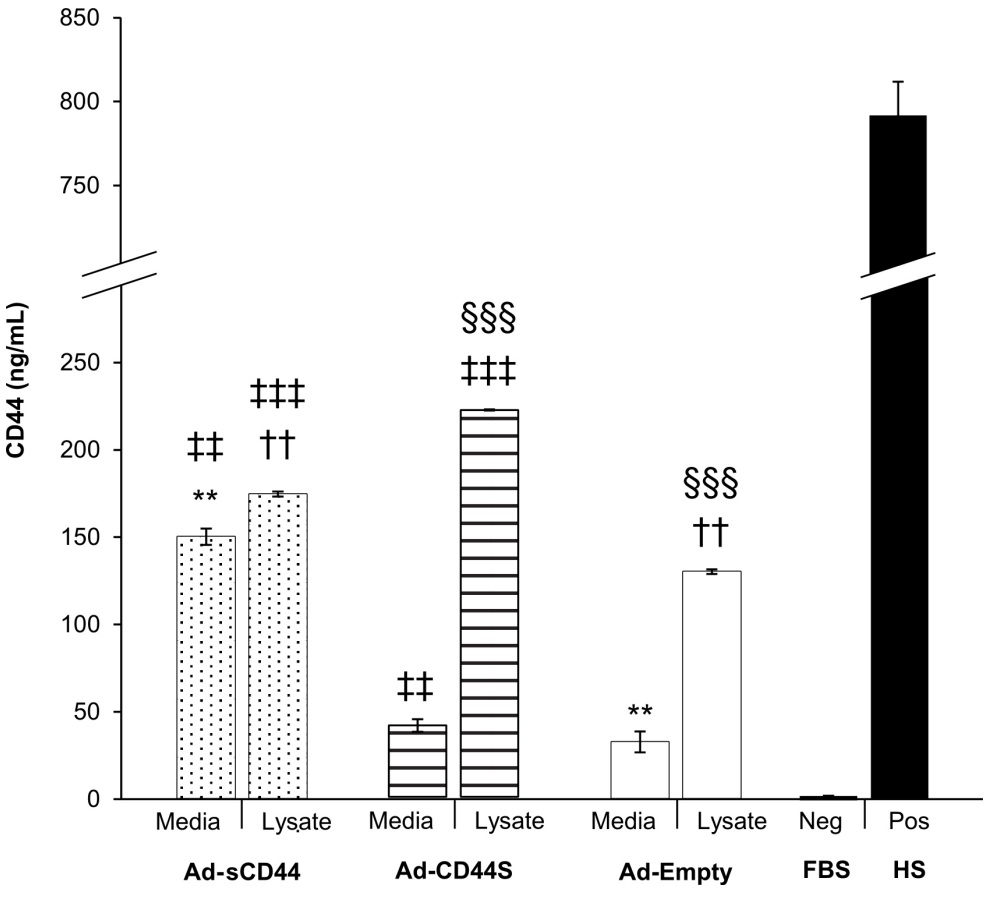

Figure 2. Effects of Ad-sCD44 and Ad-CD44S transduction on CD44 levels on day 7 in human trabecular meshwork cells. CD44 concentrations were determined by enzyme-linked immunosorbent assay (ELISA) and are expressed in ng/ml in both the adenoviral media and cell lysates. Fetal bovine serum (FBS) was used as negative (Neg) control; human serum (HS) was used as a positive (Pos) control. Data are the mean ± SEM; n=4. Analysis of variance (ANOVA) was used to determine significance between: Ad-Empty media versus Ad-sCD44 media ** $p<0.01$; Ad-Empty lysate versus Ad-sCD44 lysate, †† $p<0.01$; Ad-CD44S media versus Ad-sCD44 media, ‡‡ $p<0.01$; Ad-CD44S lysate versus Ad-sCD44 lysate, ‡‡‡ $p<0.001$; Ad-Empty lysate versus Ad-CD44S lysate, §§§ $p<0.001$.

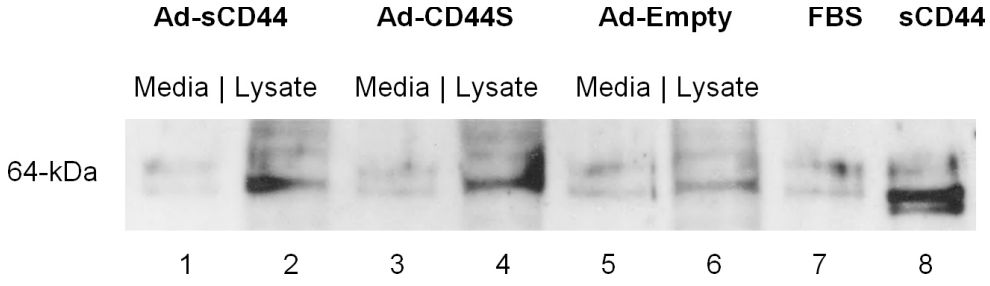

Figure 3. Effects of Ad-sCD44 and Ad-CD44S transduction on CD44 levels on day 7 in human trabecular meshwork cells. CD44 was determined by western blots of culture media and lysates of trabecular meshwork cells. The lane numbers signify the following: Lane 1, Ad-sCD44 media; lane 2, Ad-sCD44 cell lysate; lane 3, Ad-CD44s media; lane 4, Ad-CD44s cell lysate; lane5, Ad-empty media; lane 6 Ad-empty cell lysate; lane 7, fetal bovine serum (FBS) control; and lane 8, isolated 32-kDa sCD44. Western blots were performed in triplicate.

at 44 days, and remained significantly higher than control eyes. There were fewer amplitude fluctuations recorded in Ad-sCD44-treated eyes than Ad-CD44S-treated eyes. Overall, both treatments showed a prolonged, sustained increase in IOP for 50 days or longer (Figure 5).

To determine if Ad-sCD44 overexpression could be blocked by a γ-secretase inhibitor, ocular hypertension was first induced with Ad-sCD44 injection. On day 12, a 1% solution of a γ-secretase inhibitor was topically administered for 4 days. After 3 days of administration, the IOP in the γ-secretase-treated eyes significantly decreased. The IOP lowering effects of the γ-secretase inhibitor lasted an additional 2 days after the inhibitor was discontinued, and subsequently the IOP increased (Figure 6).

Anterior segment perfusion: The effects of isolated 32-kDa sCD44 were tested in anterior segment perfusion at constant pressure in porcine eyes (Figure 7). After establishing steady-state baseline flow rates, sCD44 and control perfusates were administered by anterior chamber exchange to establish time 0, and their effects were calculated as a percent change from the steady-state baseline values. In the initial 30 min from time 0, a 50% flow rate increase was observed in DMEM control perfused eyes. By 3 h, the flow reached a steady rate at approximately 20% above baseline, and maintained this rate until the 6 h time point. The time course demonstrated an increase in outflow facility in the initial 12 h of porcine perfusion with DMEM, heat-inactivated CD44, or BSA. The flow rate then continued to steadily decrease, reaching a flow rate level at an approximate negative 20% change from baseline at the 72 h time point (Figure 7). The flow rate in porcine perfusion of 1 ng/ml sCD44 was the same as the baseline flow rates. The flow rate of sCD44 observed at the 30 min time point compared to DMEM control was significantly lower ($p<0.01$). The flow rate remained at baseline until the 6 h mark and gradually declined, eventually to reach a flow rate approximately 40% below the baseline at the 72 h time

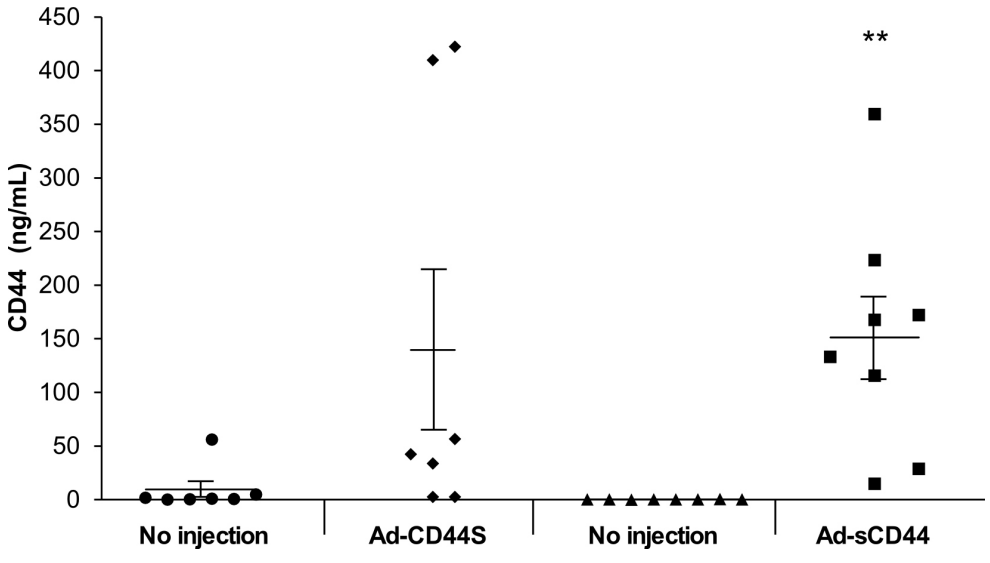

Figure 4. Enzyme-linked immunosorbent assay determination on day 14 of aqueous CD44 concentration in Ad-CD44S and Ad-sCD44 transduced mice eyes. A distribution plot of sCD44 concentration in the mouse aqueous humor is displayed for eyes treated with Ad-CD44S (n=7) or Ad-sCD44 (n=9) adenoviruses and their respective uninjected contralateral eyes. Data are expressed as mean ± SEM, **$p<0.01$, compared with the no-injection group using one-way analysis of variance (ANOVA) followed by Dunnett's test.

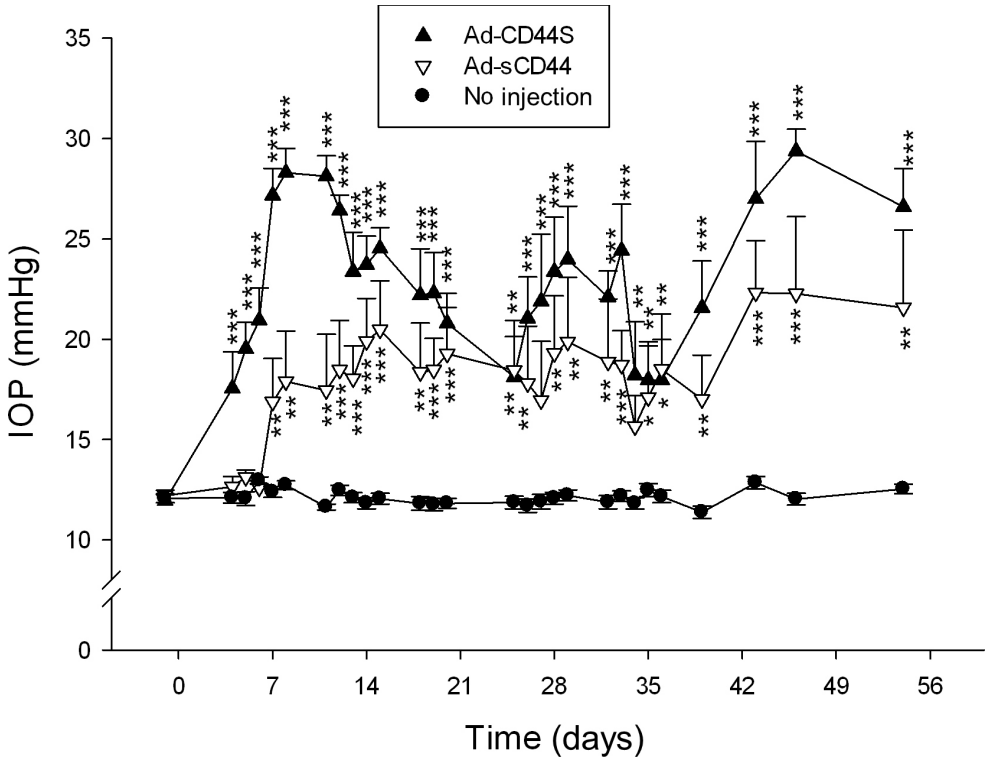

Figure 5. Effects of Ad-CD44S and Ad-sCD44 transduction on mouse intraocular pressure. One eye of BALB/cJ mice was injected intravitreally with 6×10^7 pfu with Ad-CD44S or Ad-sCD44 at day 0. The contralateral eye of mice was uninjected and served as a control. Results are expressed as mean ± SEM (n=8 for the injected groups, n=16 for control). The statistical results are: *p<0.05, **p<0.01, *** p<0.001 compared with the no-injection group using one-way analysis of variance (ANOVA) followed by Dunnett's test.

point. See Figure 7. Heat-inactivated sCD44 was similar to DMEM. Aside from a slightly less dramatic initial spike of 40% above baseline flow rate 30 min after the injection, the heat-inactivated sCD44 had a flow-rate trend nearly identical

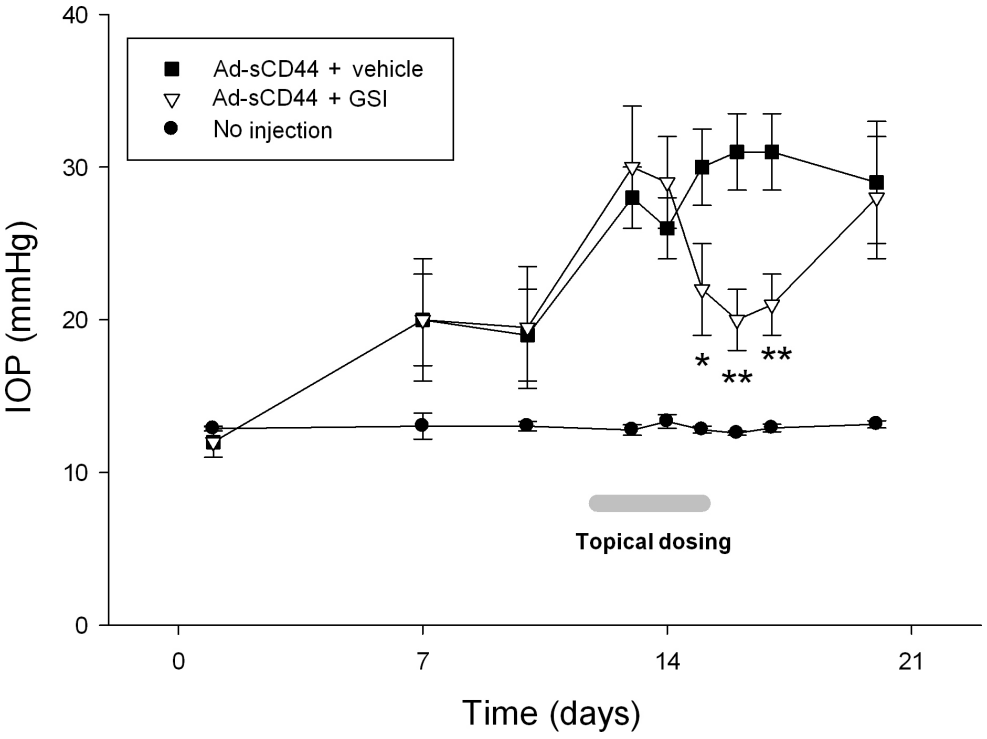

Figure 6. Effect of γ-secretase inhibitor on ocular hypertension induced by Ad-sCD44. One eye of BALB/cJ mice was injected intravitreally with 6×10^7 pfu Ad-sCD44 at day 0. The contralateral eye was uninjected. On days 12 through 15 (indicated by gray horizontal bar), a 1% solution of a γ-secretase inhibitor (GSI) or vehicle was topically applied to mice eyes. Results are expressed as mean ± SEM (n=6 for the injected groups, n=12 for control). The statistical results are: *p<0.05, **p<0.01 versus the vehicle group by Student's t-test.

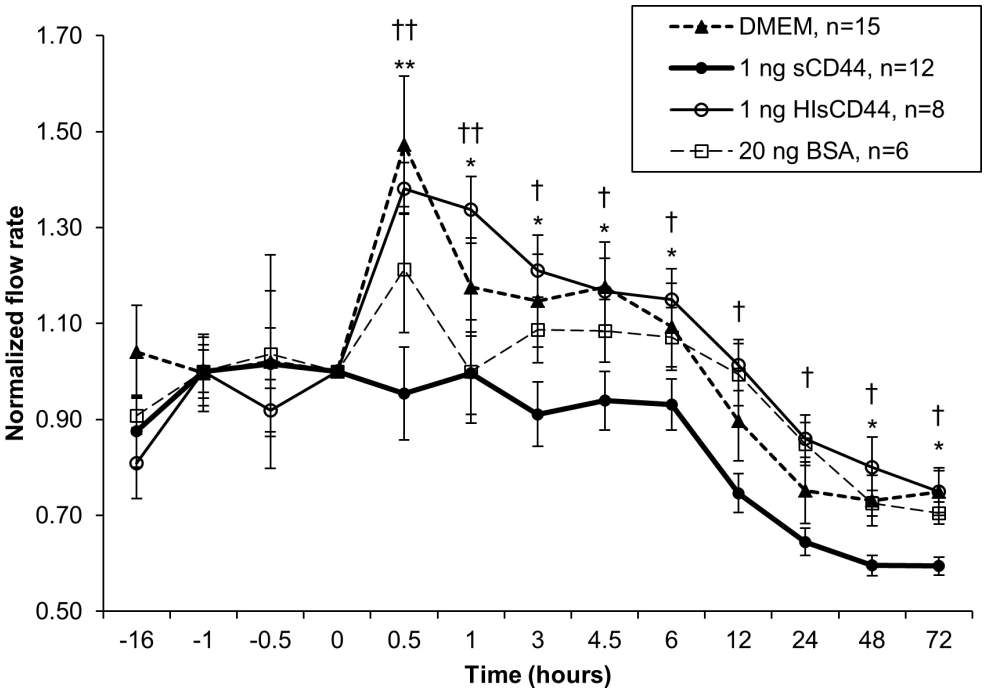

Figure 7. Effects of sCD44 on outflow rate in perfusion cultured anterior segments. After stabilization of the flow rate, time 0 represents the start of the treatment. Normalized flow rate is the percent change of the flow rate of the treated time points to average flow rate of the pre-treated time points. Porcine anterior segments were perfused at constant pressure with 1 ng/ml sCD44, 1 ng/ml heat-inactivated sCD44 (HIsCD44), 20 ng/ml BSA, or Dulbecco's Modified Eagle's Medium. Time points are the mean ± SEM and the number of experiments are shown in the insert. sCD44 versus Dulbecco's Modified Eagle's Medium (DMEM). The statistical comparisons are: sCD44 versus Dulbecco's Modified Eagle's Medium (DMEM), *p<0.05, **p<0.01; sCD44 versus HIsCD44, † p<0.05, †† p<0.01.

to that of DMEM, eventually finishing at a negative-20% baseline flow rate. BSA was similar to DMEM, although a more stable flow rate was observed in the first 12 h (Figure 7).

The flow rate effects of three different concentrations of CD44 antibody—0.5, 1.0, and 5.0 ng/ml—were measured both alone and combined with 1 ng/ml sCD44 to determine a neutralizing effect of the CD44 antibody in blocking the sCD44 effects on flow rate (Figure 8). The 0.05 ng/ml CD44 antibody concentration and 1 ng/ml sCD44 (molar ratio 1:1) behaved similarly to DMEM along a parallel pathway, with an initial peak of approximately 30% flow rate above baseline and finishing at 25% below baseline, indicating a significant neutralizing effect of sCD44. The 0.5 ng/ml CD44 antibody concentration plus 1 ng/ml sCD44 reached a delayed flow rate peak at the 1 h mark, with a modest 15% increase of the baseline measurement, and then followed a flow rate trend line just slightly above or nearly equal to that of sCD44's measurement. The 0.5 ng/ml CD44 antibody concentration and 1 ng/ml (molar ratio 10:1) was similar to 0.05 ng/ml CD44, with a slight decrease in flow rate. The 5 ng/ml CD44 antibody and 1 ng sCD44 (molar ratio 100:1) followed a flow rate trend line almost identical to that of sCD44, indicating that excess CD44 antibody acts similarly to 32-kDa sCD44 protein itself. Co-administration of a γ-secretase inhibitor with sCD44 also significantly neutralized the effect of sCD44 on flow rate. See Figure 9.

CD44 effects on trabecular meshwork cell actin organization: Structural differences in the TM cell cytoskeleton in cell culture were observed using confocal microscopy in the samples treated with 0.1 ng sCD44. The PBS control cells demonstrated normal, expected conformations of F-actin as diffuse arrangements and tightly packed stress fiber bundles (Figure 10). In contrast, TM cells treated with 0.1 ng sCD44 displayed distinct CLAN-like formations. These CLAN formations were defined by a minimum requirement of three vertices connected by three actin spokes creating a triangle in a series of geodesic dome structures.

To further explore changes in the actin cytoskeleton of 32-kDa sCD44-treated TM cells, we also examined the co-localization of annexin 2, a known modulator of the actin skeleton. Indeed, annexin 2 co-localized with actin in CLAN-like structures. An increase in the concentration of phosphorylated annexin 2, a negative modular of actin assembly, was noted in the spokes and vertices of the CLAN formations. This co-localization of F-actin and phosphorylated annexin 2 was apparent when the images of actin and phosphorylated annexin 2 were merged together, overlapping spatially on their axes (Figure 10).

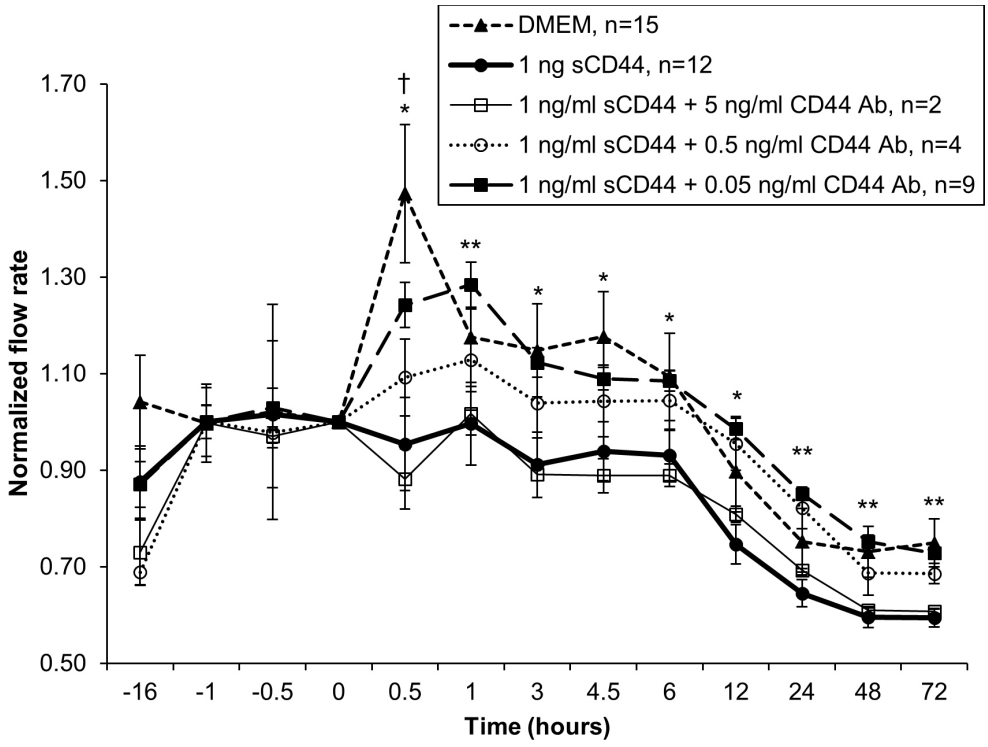

Figure 8. Effects of CD44 neutralizing antibody on sCD44 normalized flow rate. Porcine anterior segments were perfused with 1 ng/ml sCD44 (as shown in Figure 7), 1 ng/ml sCD44 + 0.05 ng/ml CD44 antibody, 1 ng/ml CD44 + 0.5 ng/ml CD44 antibody, and 1 ng/ml CD44 + 5.0 ng/ml CD44 antibody. Time points are the mean±SEM and the number of experiments are shown in the insert. sCD44 versus sCD44 + 0.05 ng/ml CD44 antibody. The statistical comparisons are: sCD44 versus sCD44 + 0.05 ng/ml CD44 antibody, *p<0.05, **p<0.01; 0.05 ng/ml CD44 antibody versus 5.0 ng/ml CD 44 antibody, † p<0.05.

To examine changes in cell cytoskeletal response to sCD44 in cell culture, the percent of F-actin that exhibited CLAN-like characteristics was analyzed in individual cells. The control group exhibited on average 97.8 normal actin vertices and 13.1 CLAN-like vertices (range of 0–32) per cell count, while the sCD44-treatment group exhibited on average

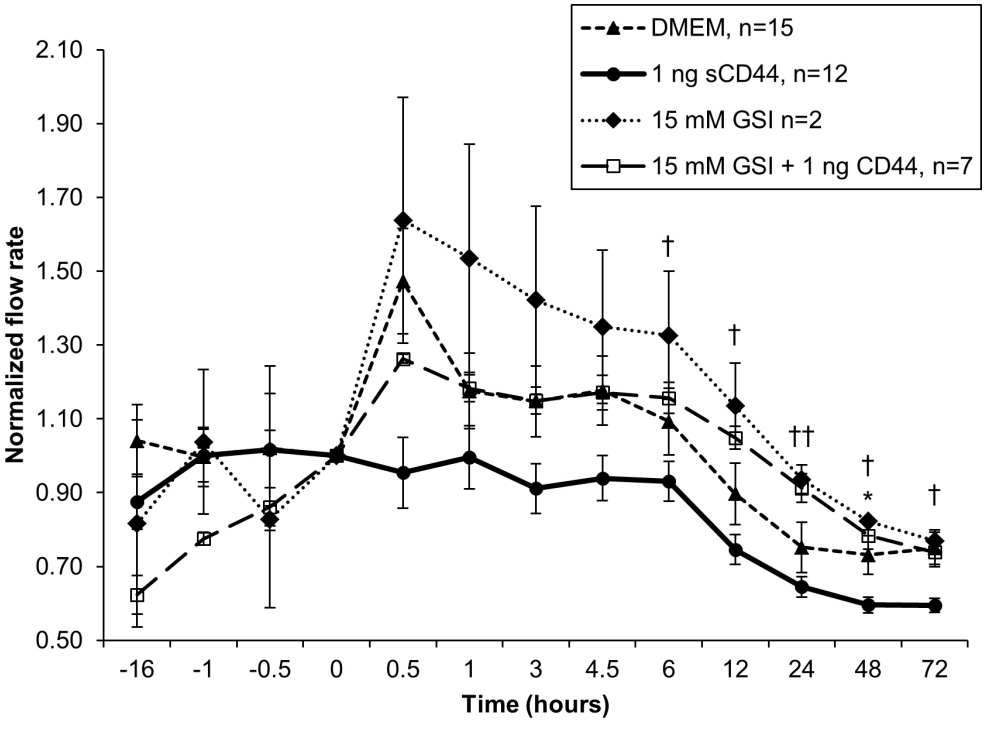

Figure 9. Effects of γ-secretase inhibitor (GSI) on sCD44 normalized flow rate in perfusion cultured porcine anterior segments. Porcine anterior segments were perfused at constant pressure with 1 ng/ml sCD44 (as shown in Figure 7), 1 ng/ml CD44 + 15 mM GSI and 15 mM GSI alone. Time points are the mean ± SEM and the number of experiments are shown in the insert. The statistical comparisons are: sCD44 versus GSI alone, *p<0.05; sCD44vsCD44 +15mM GSI, † p<0.05, †† p<0.01. DMEM is Dulbecco's Modified Eagle's Medium.

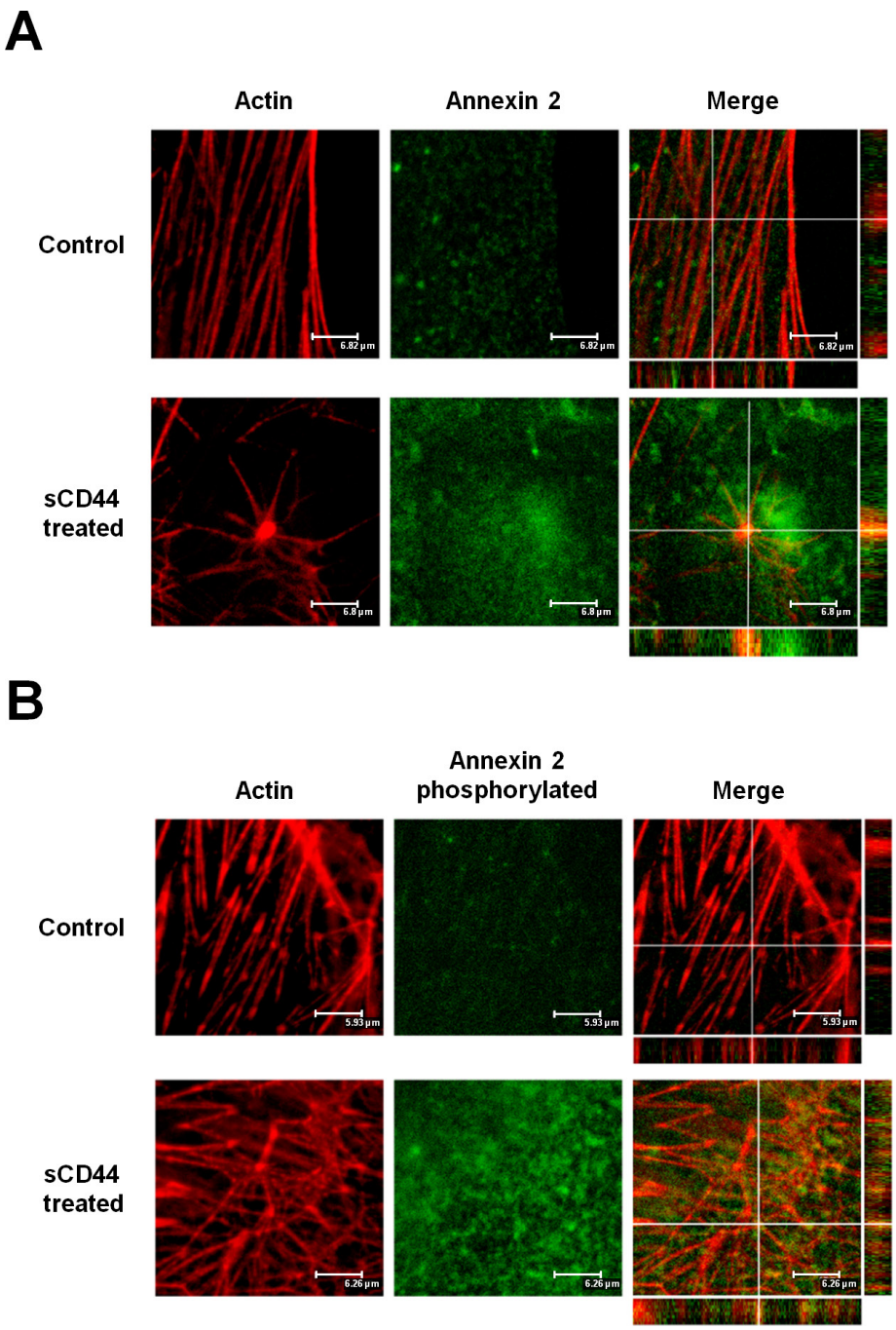

Figure 10. Confocal microscopy of sCD44-treated human trabecular meshwork cells. **A**: sCD44-treated cells were stained with rhodamine phalloidin (red) and FITC anti-annexin 2 (green). **B**: sCD44-treated cells were stained with rhodamine phalloidin and FITC anti-phosphorylated annexin 2. Noticeable structural differences were observed in the samples treated with 0.1 ng sCD44 compared to PBS controls. There was also an observed increase in the concentration of phosphorylated annexin 2 surrounding the spokes and vertices of the cross-linked actin network formations. This co-localization of F-actin and phosphorylated annexin 2 can be seen when images of the specific fluorescence of each substance were overlapped spatially on their precise axes. Magnification is 200×.

71.9 normal actin vertices and 39.8 CLAN-like vertices (range of 12–62) per cell count. The results demonstrated a significant increase ($p<0.0001$) in the percent of F-actin arranged in cross-linked actin networks in sCD44 (34.7% F-actin vertices) compared with the control group (11.5% F-actin vertices).

Table 1. Western immunoblot evaluation of annexin 2 and caveolin expression in cultured human TM cells and microdissected porcine TM tissues

Protein	Function	Human TM Cells*			Mircodissected perfused porcine TM*		
		Control (PBS)	sCD44 treated-with 0.1 ng for 24 h	Ratio	Control (DMEM)	sCD44 treated with 1 ng for 72 h	Ratio
Annexin 2	Junctional Assembly Actin Cytoskeleton Chloride Channel	109	69.2	0.63	90.6	48	0.53
Annexin 2 phosphorylated	Negative modulator of actin assembly	11	41.1	3.72	47.9	56.8	1.19
Caveolin 1	Oligomers form lipid rafts	51.4	60.2	1.17	19.9	86.2	4.34
Caveolin 2	Lipid rafts	25.6	24.2	0.95	100	89.1	0.89

Protein loading control for each western blot was GAPDH and the protein abundance is expressed as densitometric units and normalized to Jurkat cell lysate as a positive control. *in 100,000s of densitometric units annexin 2 and caveolin 2 showed decreased concentrations in human and porcine TM cells when samples were treated with sCD44. Phosphorylated annexin 2 and caveolin 1 concentrations were increased in human and porcine TM cells when treated with sCD44. Comparison of densitometric data are an estimate of relative changes in protein concentration.

Lipid raft profiles: CD44 is present in detergent-resistant, cholesterol-containing lipid rafts. The effects of sCD44-treatment on specific lipid raft protein concentrations in human TM cells and microdissected perfused porcine TM were analyzed by western blot (Table 1). Annexin 2 and caveolin 2 were both decreased when samples were treated with sCD44, with respective densitometric ratios of 0.63 and 0.95 in human TM cells and 0.53 and 0.89 in porcine TM. Phosphorylated annexin 2 and caveolin 1 were both increased when samples were treated with sCD44, with respective densitometric ratios of 3.72 and 1.17 in human TM cells and 1.19 and 4.34 in perfused porcine TM. Aside from the phosphorylated annexin 2, sCD44 treatment had a greater effect on perfused porcine TM (Table 1).

DISCUSSION

This study provides support for the role for CD44 in increased aqueous outflow resistance and elevated IOP, as well as for its multiple roles in the cell biology of the TM. Intravitreal injection of CD44 adenoviral constructs in mice showed a significant correlation between overexpression of CD44 and a sustained increase in IOP. Infusion of sCD44 in anterior segment perfusion exhibited a marked decrease in flow rates lasting 72 h. The effects of isolated sCD44 on flow rates were lessened by co-infusion of a neutralizing sCD44 antibody. These two models of CD44—an exogenous addition of isolated 32-kDa sCD44 to perfused organ cultures and overexpression by Ad-CD44 and Ad-sCD44 injection into mouse eyes—clearly demonstrate an effect of CD44 on IOP. The exogenous model of sCD44 reduced outflow was rapid within 30 min, suggesting a CD44 receptor effect, a cell-signaling effect, or perhaps an extracellular matrix effect. In contrast, the adenoviral overexpression of Ad-CD44S in mouse eyes appeared to elevate IOP within several days. The difference in timing between the quick effect of exogenous 32-kDa sCD44 and the rather slow effect of adenoviral overexpression is the outcome of multiple factors, i.e., species variability, method, in vitro versus in vivo, and most importantly, the amount and timing of the delivery of dose. Nonetheless, both the exogenous administration and adenoviral overexpression resulted in increased IOP and outflow resistance.

Exactly why overexpression of sCD44 in the mouse eye leads to increased IOP is unknown. Likewise, the mechanism underlying the effects of exogenous sCD44 on flow rates in perfused porcine eyes is unclear. It is well recognized that sCD44 is released by proteolytic cleavage of CD44 receptor upon ligand binding [24]. sCD44 binds homotypically to itself and to its CD44 receptor. As CD44 is shed, it forms protein aggregates, particularly in monomeric and oligomeric conformations. Although low concentrations of neutralizing CD44 antibody blocked the effect of exogenous 32-kDa CD44, at a higher concentration of neutralizing CD44 antibody, there is an excess of antibody. Since both exogenous sCD44 and CD44 antibody act as ligands to the CD44 receptor, in effect then, both disrupt CD44 receptor function. In addition, sCD44 appears to induce CLANs by disrupting the actin cytoskeleton. As sCD44 is shed, the remaining CD44 receptor is further processed by γ-secretase to generate an

intracytoplasmic domain that acts as a transcription factor to cause further synthesis of CD44 receptor [17]. This cascade of events leads to a positive feedback loop causing additional shedding of sCD44 so that the process is self-propagating. Therefore, exogenous sCD44 or adenoviral overexpression of sCD44 leads to increased CD44 expression. For both sCD44 and Ad-sCD44 models, as well as in the vitreous model recently reported by the Ildefonso group [25], the sCD44 levels were blocked by γ-secretase inhibition, further supporting the notion of a positive feedback loop.

Adenoviral constructs and their effect on IOP have been used successfully in studying TGFβ1 [26], TGFβ2 [18], SPARC [27], SFRP1 [28], serum amyloid A [29], PEDF [30], caldesmon [31], and myocilin [32]. CD44 serves as a co-receptor, linking signaling receptors such as c-Met, members of the ErbB family of receptor tyrosine kinases, transforming growth factor-β (TGF-β) receptors, and hepatocyte growth factor, as well as facilitating the association of intracellular mediators of signal transduction [33]. Overexpression and proteolytic release of sCD44 by cells interfere with HA binding to CD44, resulting in sCD44 acting as a decoy receptor to all available binding of endogenous HA [33]. Moreover, CD44 antibody also binds the CD44 receptor, leading to mitochondrial dysfunction and cell death [34]. We have previously shown that sCD44 binds homotypically to CD44 [20]. It is then internalized via clathrin-independent endocytosis [35]. After internalization, CD44 releases an intracellular domain that is trafficked either to the nucleus [17] or to the mitochondria [20], depending on the γ-secretase cleavage site.

In the human TM cell culture, sCD44 administration modified the actin cytoskeleton by increasing the formation of actin arrangements known as CLANs. Dexamethasone [36] and TGF β2 [37] have been shown to induce CLAN formation in TM cells. Annexin 2 is known to have a close relationship with F-actin, serving to bind and bundle it through a tetrameric complex [38]. Specifically, the C-terminus of annexin 2 has been shown to mediate binding to F-actin [39]. Experimental evidence shows that annexin 2 localizes to regions of actin where there are free-barbed ends [40], and it has been suggested that annexin 2 may serve as a barbed-end-capping protein that restricts actin growth and motility [41]. From our experimental results, sCD44 shifted the equilibrium of annexin 2 toward its phosphorylated form, with a corresponding increase in CLAN formation. We hypothesize that phosphorylation of annexin 2 induced by sCD44 impedes the ability of annexin 2 to cap barbed ends and allows additional outward growth, resulting in increased actin spokes and the formation of CLANS. The time course demonstrated an increase in outflow facility in the initial 12 h of porcine perfusion with DMEM, heat-inactivated CD44, or BSA. This phenomenon in aqueous outflow is commonly referred to as "washout" [42] and occurs in all eyes of all species other than humans. The initial increase in flow rate in our porcine perfusion may be caused by anterior chamber exchange, the volume of the perfusate, the use of magnetic stir bars to ensure uniform distribution of a test substance, species variability, or cellular matrix alterations. The observation that sCD44 prevents the initial high flow rate suggests the CD44 acts rather quickly on the outflow mechanism. The addition of exogenous 32-kDa CD44 in this study prevented an increase in flow facility. CD44 binds to HA, providing resistance to shear forces on the surface of endothelial cells [43] and promoting vascular integrity [44]. In addition, the observation of CLAN formation in perfused porcine TM cells suggests than the TM endothelial cells are less pliable and rigid [45], which would prevent their separation from their basal lamina. Taken together, exogenous CD44 acts to prevent the washout phenomenon.

Our results from using adenoviral overexpression of sCD44 and organ perfusion of sCD44 indicate that sCD44 decreases aqueous outflow rates, with a subsequent increase in IOP. In both models, the effects of overexpression of sCD44 were blocked by inhibiting CD44 proteolysis with a γ-secretase inhibitor. Our in vitro results also indicate sCD44 increased TM-cell CLAN formation and changed annexin 2 and caveolin protein concentrations in lipid rafts. The elevated sCD44 levels seen in POAG aqueous may play causative roles in POAG pathogenesis.

ACKNOWLEDGMENTS

Supported by BrightFocus Foundation Grant G2011–047, National Eye Institute Grants RO1EY12043 and P30EY01792, Alcon Research, Ltd, Fort Worth, Texas, Rosemary O'Meara and Kathleen F. Connelly Memorial Funds, Illinois Society for the Prevention of Blindness, Midwest Eye-Banks and Transplantation Center, and an unrestricted grant from the Research to Prevent Blindness.

REFERENCES

1. Weinreb RN, Khaw PT. Primary open-angle glaucoma. Lancet 2004; 363:1711-20. [PMID: 15158634].

2. Knepper PA, Mayanil CS, Goossens W, Wertz RD, Holgren C, Ritch R, Allingham RR. Aqueous humor in primary open-angle glaucoma contains an increased level of CD44S. Invest Ophthalmol Vis Sci 2002; 43:133-9. [PMID: 11773023].

3. Nolan MJ, Giovingo MC, Miller AM, Wertz RD, Ritch R, Liebmann JM, Allingham RR, Herndon LW, Wax MB,

Smolyak R, Hasan F, Barnett EM, Samples JR, Knepper PA. Aqueous humor sCD44 concentration and visual field loss in primary open-angle glaucoma. J Glaucoma 2007; 16:419-29. [PMID: 17700283].

4. Choi J, Miller AM, Nolan MJ, Yue BY, Thotz ST, Clark AF, Agarwal N, Knepper PA. sCD44 is cytotoxic to trabecular meshwork and retinal ganglion cells in vitro. Invest Ophthalmol Vis Sci 2005; 46:214-22. [PMID: 15623776].

5. Zöller M. CD44: can a cancer-initiating cell profit from an abundantly expressed molecule? Nat Rev Cancer 2011; 11:254-67. [PMID: 21390059].

6. Kincade PW, Zheng Z, Katoh S, Hanson L. The importance of cellular environment to function of the CD44 matrix receptor. Curr Opin Cell Biol 1997; 9:635-42. [PMID: 9330866].

7. Cichy J, Pure E. The liberation of CD44. J Cell Biol 2003; 161:839-43. [PMID: 12796473].

8. Naor D, Sionov RV, Ish-Shalom D. CD44: structure, function, and association with the malignant process. Adv Cancer Res 1997; 71:241-319. [PMID: 9111868].

9. Knepper PA, Samples JR, Yue BYJT. Biomarkers of primary open-angle glaucoma. Expert Rev Ophthalmol 2010; 5:731-42. .

10. Naor D, Nedvetzki S, Walmsley M, Yayon A, Turley EA, Golan I, Caspi D, Sebban LE, Zick Y, Garin T, Karussis D, Assayag-Asherie N, Raz I, Weiss L, Slavin S, Golan I. CD44 involvement in autoimmune inflammations: the lesson to be learned from CD44-targeting by antibody or from knockout mice. Ann N Y Acad Sci 2007; 1110:233-47. [PMID: 17911438].

11. Vachon E, Martin R, Kwok V, Cherepanov V, Chow CW, Doerschuk CM, Plumb J, Grinstein S, Downey GP. CD44-mediated phagocytosis induces inside-out activation of complement receptor-3 in murine macrophages. Blood 2007; 110:4492-502. [PMID: 17827392].

12. Ghatak S, Misra S, Toole BP. Hyaluronan oligosaccharides inhibit anchorage-independent growth of tumor cells by suppressing the phosphoinositide 3-kinase/Akt cell survival pathway. J Biol Chem 2002; 277:38013-20. [PMID: 12145277].

13. Hegde VL, Singh NP, Nagarkatti PS, Nagarkatti M. CD44 mobilization in allogeneic dendritic cell-T cell immunological synapse plays a key role in T cell activation. J Leukoc Biol 2008; 84:134-42. [PMID: 18388297].

14. Naor D, Wallach-Dayan SB, Zahalka MA, Sionov RV. Involvement of CD44, a molecule with a thousand faces, in cancer dissemination. Semin Cancer Biol 2008; 18:260-7. [PMID: 18467123].

15. Kajita M, Itoh Y, Chiba T, Mori H, Okada A, Kinoh H, Seiki M. Membrane-type 1 matrix metalloproteinase cleaves CD44 and promotes cell migration. J Cell Biol 2001; 153:893-904. [PMID: 11381077].

16. Seiki M. The cell surface: the stage for matrix metalloproteinase regulation of migration. Curr Opin Cell Biol 2002; 14:624-32. [PMID: 12231359].

17. Lammich S, Okochi M, Takeda M, Kaether C, Capell A, Zimmer AK, Edbauer D, Walter J, Steiner H, Haass C. Presenilin-dependent intramembrane proteolysis of CD44 leads to the liberation of its intracellular domain and the secretion of an Aβ-like peptide. J Biol Chem 2002; 277:44754-9. [PMID: 12223485].

18. Shepard AR, Millar JC, Pang IH, Jacobson N, Wang WH, Clark AF. Adenoviral gene transfer of active human transforming growth factor-β2 elevates intraocular pressure and reduces outflow facility in rodent eyes. Invest Ophthalmol Vis Sci 2010; 51:2067-76. [PMID: 19959644].

19. Wang WH, Millar JC, Pang IH, Wax MB, Clark AF. Noninvasive measurement of rodent intraocular pressure with a rebound tonometer. Invest Ophthalmol Vis Sci 2005; 46:4617-21. [PMID: 16303957].

20. Nolan MJ, Koga T, Walker L, McCarty R, Grybauskas A, Giovingo MC, Skuran K, Kuprys PV, Knepper PA. sCD44 internalization in human trabecular meshwork cells. Invest Ophthalmol Vis Sci 2013; 54:592-601. [PMID: 23287794].

21. Bradley JMB, Vranka J, Colvis CM, Conger DM, Alexander JP, Fisk AS, Samples JR, Acott TS. Effect of matrix metalloproteinases activity on outflow in perfused human organ culture. Invest Ophthalmol Vis Sci 1998; 39:2649-58. [PMID: 9856774].

22. Keller KE, Bradley JM, Kelley MJ, Acott TS. Effects of modifiers of glycosaminoglycan biosynthesis on outflow facility in perfusion culture. Invest Ophthalmol Vis Sci 2008; 49:2495-505. [PMID: 18515587].

23. Stamer WD, Seftor RE, Williams SK, Samaha HA, Synder RW. Isolation and culture of trabecular meshwork cells by extracellular matrix digestion. Curr Eye Res 1995; 14:611-7. [PMID: 7587308].

24. Stamenkovic I, Yu Q. Shedding light on proteolytic cleavage of CD44: the responsible sheddase and functional significance of shedding. J Invest Dermatol 2009; 129:1321-4. [PMID: 19434087].

25. Ildefonso CJ, Bond WS, Al-Tawashi AR, Hurwitz MY, Hurwitz RL. The liberation of CD44 intracellular domain modulates adenoviral vector transgene expression. J Biol Chem 2012; 287:32697-707. [PMID: 22865879].

26. Robertson JV, Golesic E, Gauldie J, West-Mays JA. Ocular gene transfer of active TGF-β induces changes in anterior segment morphology and elevated IOP in rats. Invest Ophthalmol Vis Sci 2010; 51:308-18. [PMID: 19696167].

27. Oh DJ, Kang MH, Choi KR, Sage EH, Rhee DJ. Adenoviral gene transfer of SPARC to human trabecular meshwork elevates intraocular pressure. Paper presented at: The ARVO Annual Meeting; May 4, 2011; Fort Lauderdale, FL.

28. Wang WH, McNatt LG, Pang IH, Millar JC, Hellberg PE, Hellberg MH, Steely HT, Rubin JS, Fingert JH, Sheffield VC, Stone EM, Clark AF. Increased expression of the WNT antagonist sFRP-1 in glaucoma elevates intraocular pressure. J Clin Invest 2008; 118:1056-64. [PMID: 18274669].

29. Wang WH, McNatt LG, Pang IH, Hellberg PE, Fingert JH, McCartney MD, Clark AF. Increased expression of serum amyloid A in glaucoma and its effect on intraocular pressure. Invest Ophthalmol Vis Sci 2008; 49:1916-23. [PMID: 18223246].

30. Yokoi K, Zhang HS, Kachi S, Balaggan KS, Yu Q, Guschin D, Kunis M, Surosky R, Africa LM, Bainbridge JW, Spratt SK, Gregory PD, Ali RR, Campochiaro PA. Gene transfer of an engineered zinc finger protein enhances the anti-angiogenic defense system. Mol Ther 2007; 15:1917-23. [PMID: 17700545].

31. Gabelt BT, Hu Y, Vittitow JL, Rasmussen CR, Grosheva I, Bershadsky AD, Geiger B, Borrás T, Kaufman PL. Caldesmon transgene expression disrupts focal adhesions in HTM cells and increases outflow facility in organ-cultured human and monkey anterior segments. Exp Eye Res 2006; 82:935-44. [PMID: 16442523].

32. Borrás T, Bryant PA, Chisolm SS. First look at the effect of overexpression of TIGR/MYOC on the transcriptome of the human trabecular meshwork. Exp Eye Res 2006; 82:1002-10. [PMID: 16476427].

33. Knudson CB, Knudson W. Hyaluronan-binding proteins in development, tissue homeostasis, and disease. FASEB J 1993; 7:1233-41. [PMID: 7691670].

34. Rajasagi M, von Au A, Singh R, Hartmann N, Zöller M, Marhaba R. Anti-CD44 induces apoptosis in T lymphoma via mitochondrial depolarization. J Cell Mol Med 2010; 14:1453-67. [PMID: 19765170].

35. Howes MT, Kirkham M, Riches J, Cortese K, Walser PJ, Simpson F, Hill MM, Jones A, Lundmark R, Lindsay MR, Hernandez-Deviez DJ, Hadzic G, McCluskey A, Bashir R, Liu L, Pilch P, McMahon H, Robinson PJ, Hancock JF, Mayor S, Parton RG. Clathrin-independent carriers form a high capacity endocytic sorting system at the leading edge of migrating cells. J Cell Biol 2010; 190:675-91. [PMID: 20713605].

36. Clark AF, Brotchie D, Read AT, Hellberg P, English-Wright S, Pang IH, Ethier CR, Grierson I. Dexamethasone alters F-actin architecture and promotes cross-linked actin network formation in human trabecular meshwork tissue. Cell Motil Cytoskeleton 2005; 60:83-95. [PMID: 15593281].

37. O'Reilly S, Pollock N, Currie L, Paraoan L, Clark AF, Grierson I. Inducers of cross-linked actin networks in trabecular meshwork cells. Invest Ophthalmol Vis Sci 2011; 52:7316-24. [PMID: 21849423].

38. Gerke V, Weber K. Identity of p36K phosphorylated upon Rous sarcoma virus transformation with a protein purified from brush borders; calcium-dependent binding to non-erythroid spectrin and F-actin. EMBO J 1984; 3:227-33. [PMID: 6323166].

39. Filipenko NR, Waisman DM. The C-terminus of annexin II mediates binding to F-actin. J Biol Chem 2001; 276:5310-5. [PMID: 11067857].

40. Hayes MJ, Shao D, Bailly M, Moss SE. Regulation of actin dynamics by annexin 2. EMBO J 2006; 25:1816-26. [PMID: 16601677].

41. Hayes MJ, Merrifield CJ, Shao D, Ayala-Sanmartin J, Schorey CD, Levine TP, Proust J, Curran J, Bailly M, Moss SE. Annexin 2 binding to phosphatidylinositol 4,5-bisphosphate on endocytic vesicles is regulated by the stress response pathway. J Biol Chem 2004; 279:14157-64. [PMID: 14734570].

42. Scott PA, Lu Z, Liu Y, Gong H. Relationships between increased aqueous outflow facility during washout with the changes in hydrodynamic pattern and morphology in bovine aqueous outflow pathways. Exp Eye Res 2009; 89:942-9. [PMID: 19679123].

43. Nandi A, Estess P, Siegelman MH. Hyaluronan anchoring and regulation on the surface of vascular endothelial cells is mediated through the functionally active form of CD44. J Biol Chem 2000; 275:14939-48. [PMID: 10809739].

44. Lennon FE, Singleton PA. Hyaluronan regulation of vascular integrity. Am J Cardiovasc Dis. 2011; 1:200-13. [PMID: 22254199].

45. Last JA, Pan T, Ding Y, Reilly CM, Keller K, Acott TS, Fautsch MP, Murphy CJ, Russell P. Elastic modulus determination of normal and glaucomatous human trabecular meshwork. Invest Ophthalmol Vis Sci 2011; 52:2147-52. [PMID: 21220561].

46. Legg JW, Lewis CA, Parson M, Ng T, Isacke CM. A novel PKC-regulated mechanism controls CD44 ezrin association and directional cell motility. Nat Cell Biol 2002; 4:399-407. [PMID: 12032545].

47. Tzircotis G, Thorne RF, Isacke CM. Directional sensing of a phorbol ester gradient requires CD44 and is regulated by CD44 phosphorylation. Oncogene 2006; 25:7401-10. [PMID: 16785995].

48. Isacke CM, Yarwood H. The hyaluronan receptor, CD44. Int J Biochem Cell Biol 2002; 34:718-21. [PMID: 11950588].

Articles are provided courtesy of Emory University and the Zhongshan Ophthalmic Center, Sun Yat-sen University, P.R. China. The print version of this article was created on 1 November 2013. This reflects all typographical corrections and errata to the article through that date. Details of any changes may be found in the online version of the article.